

ESTIMATION OF INTERFACE LOADS BY MULTI-BODY DYNAMICS SIMULATION/MODELING AND VALIDATION WITH FLIGHT TEST DATA

H. König*, M. Minciotti*

* Airbus Helicopters Deutschland GmbH - Industriestraße 4 - 86609 Donauwörth - Germany

Corresponding Author:

E-mail: hagen.koenig@airbus.com - Phone: +49 (0) 906 71 8533
mattia.minciotti@airbus.com - Phone: +49 (0) 906 71 9154

Abstract

In rotorcrafts, the control system of the main rotor is a complex assembly subjected to high dynamic loads, strongly depending on blade aerodynamics and flight maneuvers. In early development phase, loads at pitch control rods are traditionally estimated from past experience, based on the most critical maneuver of existing similar rotor systems and validated only at a later stage by flight test. As a result, in order to cover the whole flight envelope with sufficient confidence, loads in early development phase are usually very conservative and do not allow for accurate fatigue analysis of the different components of the control system.

To improve the accuracy of load prediction for the control system of new helicopters in the early design phase, interface loads for the main components of the flight control system have to be estimated based on blade loads and different swash plate positions, corresponding to different flight maneuvers.

In this paper, loads in the power boosted flight control system of a medium-size helicopter, resulting from different maneuvers are estimated through Computer Aided Engineering (CAE) by means of a kinematic model, taking into account the elastic stiffness of single components and joints.

The analysis is performed using the Multi Body Dynamics (MBD) software MotionSolve, and the main components in the control chain are represented as flexible bodies. The flexible bodies are used to account for the elasticity of bodies in MBD simulation. The technique to generate a flexible body is called Component Mode Synthesis (CMS) and consists in reducing a Finite Element Method (FEM) model of an elastic body to the interface degrees of freedom and a set of normal modes. The flexible bodies are generated using the FEM solver Optistruct. The whole methodology is validated by comparison with the test data of existing flight-measurement campaigns.

Thanks to this approach, it is possible to accurately predict the interface control loads, system stiffness and avoid excessive deflections in early design phase, leading to both reduced development time and flight test effort. In addition, this method allows for weight optimization by taking into account fatigue and fail-safe requirements already in early design phase.

This approach will be applied to the future development projects at AHD¹ and may be used as well for eventual incident investigations, resulting in reduced processing time.

¹ Airbus Helicopters Deutschland GmbH

1. INTRODUCTION.....	2
1.1 Upper Control.....	2
1.2 Bluecopter Demonstrator.....	2
2. METHODOLOGY.....	2
2.1 Multi Body Dynamics approach.....	2
2.2 Model overview	3
2.3 Generation of Flexible Bodies	4
3. RESULTS AND VALIDATION.....	5
3.1 Selected flight maneuvers	5
3.2 Comparison of Measurement Results and Calculated Data.....	5
4. CONCLUSION	9
5. REFERENCES.....	9

1. INTRODUCTION

1.1 Upper Control

In rotorcrafts, the flight control system is a complex assembly subjected to high dynamic loads, strongly depending on blade aerodynamics and flight maneuvers.

The control inputs from the pilot are transferred via control rods to the hydraulic unit, where they are boosted and routed to the mixing lever assembly. The mixing lever assembly transfers the inputs to the swash plate and from there directly to the main rotor blade.

The main rotor upper control assembly is a key feature in a rotorcraft. As an eventual loss of any of its components may result in a catastrophic failure, particular care shall be taken during sizing and every component shall be designed to ensure the highest reliability in any flight condition.

1.2 Bluecopter Demonstrator

The Bluecopter Demonstrator (BD) is a prototype helicopter developed at AHD to prove the feasibility of future eco-friendly helicopter concepts and to demonstrate “green” technologies in-flight. The main objectives of the demonstrator are (Ref. [1]):

- significant reduction in CO₂ emission and fuel consumption up to 40%;
- noise reduction of around 10 EPNdB below the ICAO noise certification limits.

The BD is based on a light/medium twin engine helicopter (EC135 S01) used as a test bed for a set of innovative and widely patented technologies. A major

contribution to the improved efficiency and minimized acoustic emission of the BD is provided by the newly developed rotor system. It includes an innovative five-bladed bearingless main rotor with increased diameter, a BlueEdge™ style blade shape, a new twist distribution, new eco optimized airfoils and a low tip speed design. Moreover it features an advanced Fenestron with an optimized blade and stator design.

The BD has been successfully tested in flight in 2014 and 2015. More information and details about the Bluecopter technologies and the achieved benefits in terms of performance and acoustic emission can be found in Ref. [1].

In this paper, loads in the power boosted flight control system of Bluecopter Demonstrator, resulting from different maneuvers are estimated using Computer Aided Engineering (CAE) by means of a kinematic model, taking into account the elastic stiffness of single components and joints.

2. METHODOLOGY

The methodology shown in this paper is based on dynamic transient analyses based on the Multi Body Dynamics (MBD) approach. In addition, Component Mode Synthesis (CMS) has been introduced to account for flexible bodies (or flexbodies).

2.1 Multi Body Dynamics approach

MBD refers to a mechanical system made of several rigid bodies (i.e. masses and inertias) linked together by different types of joints, which allow relative motions between the bodies. Joints may allow relative motion (i.e. translations and rotations) along the prescribed directions and preclude it in other ones.

In order to overcome the limitations given by the usage of rigid bodies, flexible bodies can be introduced instead. A flexbody is a representation of a component with realistic mass and stiffness distribution and it is usually generated by Finite Element Method (FEM) calculations through modal synthesis methods.

An MBD model is therefore composed by-bodies (either rigid or flexible), joints, external forces and imposed motions.

The dynamic analysis is performed by integrating a system of differential non-linear equation according to Newton's second law of motion. The system of equations to be solved can be written in compact form as:

$$(1) \quad [M]\{\ddot{u}\} + [C]\{\dot{u}\} + [K]\{u\} = \{F(t)\}$$

where $\{u(t)\}$ is the generalized displacement vector and $[M(t)], [C(t)], [K(t)]$ are respectively the mass, damping and stiffness matrices of the system which are changing over time as well.

The system of equations in described by Eq. (1) shall be integrated to obtain the time-history solution for the displacements, velocities, accelerations, and internal reaction forces in response to the set of applied forces $\{F(t)\}$. As this paper focuses on steady flight states only, displacements and forces are assumed to be constant over time for a given azimuthal position.

The governing equations for such an analysis are typically nonlinear, ordinary second order differential-algebraic equations (DAE). Due to their non-linearity, the equations cannot be solved analytically and shall be integrated by numerical methods.

For this study the software MotionSolve from Altair was chosen due to its flexibility and its direct connection to FEM pre-processor and solver.

2.2 Model overview

The MBD model of the upper control of the Bluecopter main rotor is shown in Figure 1. It represents the flight control system from the vertical booster rods up to the blade control cuffs and consists of 30 bodies (either rigid or flexible) and 48 joints. A flowchart of the different bodies and joints included in the MBD model is shown in Figure 2, where the flexbodies (i.e. bearing ring, control levers and control fork) are marked in red.

The main rotor is driven by the rotor mast, where a constant rotational speed (relative to 100% rpm) is applied during one or more revolutions. The five rotor blade cuffs are fixed to the rotor mast which is also attached to the rotating part of the upper control via the driving link. Each control cuff is connected to its pitch link (i.e. the rotating control rod which sets the blade pitch angle) by a spherical joint. Main rotor blades are not included in the model, as it is common practice at AHD to measure the loads directly at the pitch links. During flight test, loads at the pitch links are obtained from strain gauge measurements for different maneuvers. The measured force of one pitch link is applied to the five pitch links in the MBD model with a phase shift of 72°.

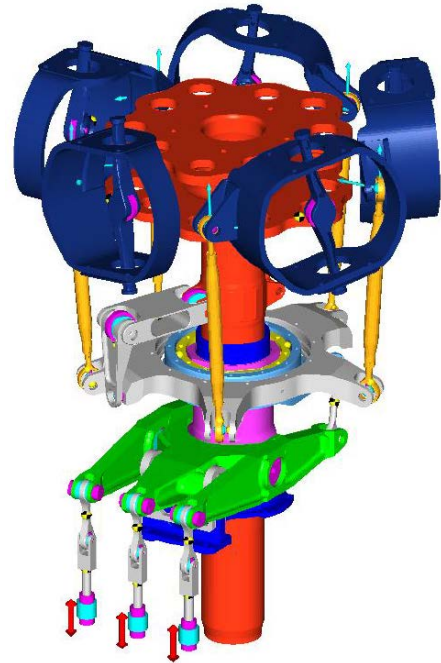


Figure 1: MBD model of Bluecopter upper control

Each pitch link is attached to the bearing ring (i.e. the rotating part of the swashplate) by a spherical joint. The bearing ring is driven in rotation by the rotor mast through one driving link assy. This “compass-like” assy allows for different swashplate positions and angles, depending on the maneuver and on the corresponding flight control inputs.

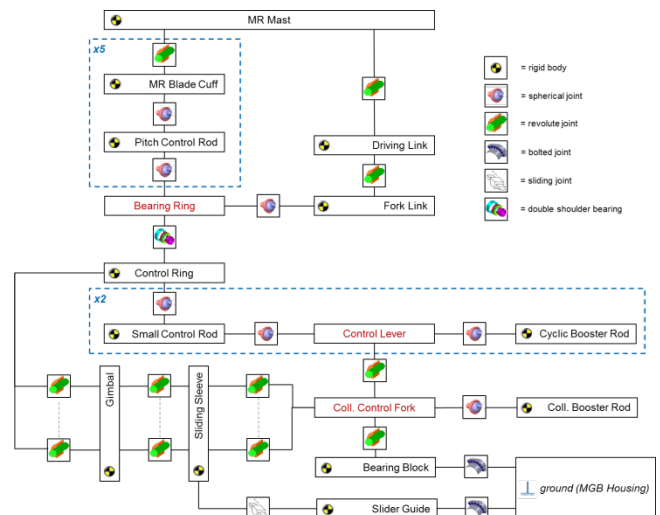


Figure 2: Sketch of the MBD model

The bearing ring runs on the control ring (i.e. the stationary part of the swashplate). This interface is represented as a frictionless cylindrical joint in the MBD model. The control ring can pivot around its mid axis and translate along the slider guide.

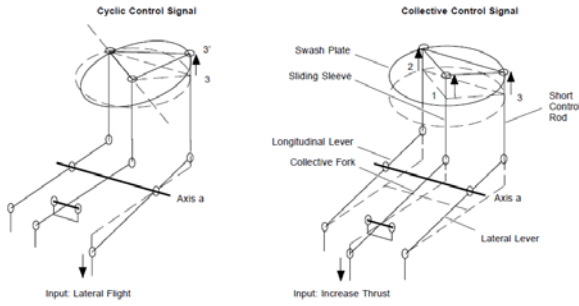


Figure 3: Schematic drawing of transmission of cyclic and collective control input signal

The cyclic control levers can pivot around the axis of the bolts connecting the levers to the collective control fork, while the fork itself can pivot around the bearing block. Both bearing block and slider guide are rigidly fixed to the main gear box housing by bolts (the main gear box housing and its attachment to the airframe are not modeled and replaced by the ground body).

As shown in Figure 3, an input in the cyclic control results in an inclination of the swashplate, while an input in the collective control affects the complete mixing lever unit (i.e. the two cyclic control levers and the collective control fork) and results in a vertical translation of the swashplate.

2.3 Generation of Flexible Bodies

The following parts are modeled as flexbodies in the upper control MBD model: cyclic lateral control lever, collective control fork, cyclic longitudinal control lever, swashplate bearing ring.

For each part, the generation of flexbodies follows three main steps:

- 1) creating a FEM mesh from CAD data;
- 2) performing a modal analysis and a CMS according to Craig-Bampton method (i.e. creating a reduced modal basis of the component);
- 3) connecting the flexbody to the existing joints in the MBD model.

The FEM meshes were created based on tetra elements. Interface nodes which will later be linked to the joints in the MBD model are connected to the mesh by means of rigid RBE2 spiders. The FEM model remains unconstrained.

Based on the unconstrained FEM model, a “free-free” modal analysis is performed, from which the first 20 resulting eigenmodes are retained. The first six modes are rigid body modes and are turned off.

In addition, for every degree of freedom (dof) at the interface nodes, static modes (i.e. static deformation states) are calculated.

Eigenmodes and static deformation states are combined in order to obtain a reduced set of orthogonal mode shapes. This set of mode shapes forms the reduced modal basis which represents the flexible body in the MBD model. Details about the CMS method and Craig-Bampton approach can be found in Ref. [2] and [3]. The first 6 non-rigid body modes of the CMS modal basis are shown in Figure 4 for the cyclic control lever.

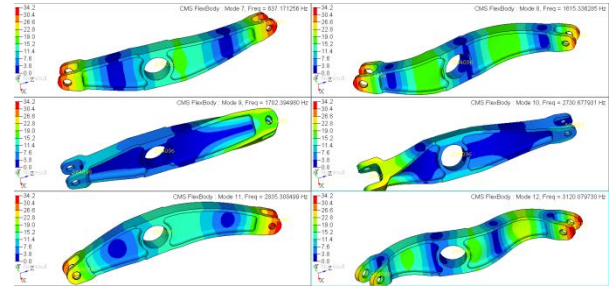


Figure 4: Normal CMS mode of cyclic control lever

The first 6 non-rigid body modes of the CMS modal basis are shown in Figure 5 for the collective control fork.

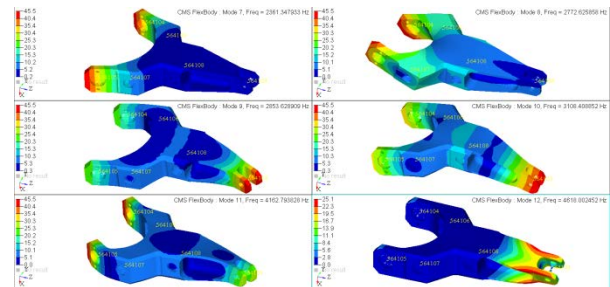


Figure 5: Normal CMS mode of cyclic control lever

The link between nodal displacement and modal shape is shown in Eq. (2); where $[\Phi_i(x, y, z)]$ is the matrix containing the reduced modal basis, which is constant over the time integration, and $\{q_i(t)\}$ is the vector of displacement in modal coordinates.

$$(2) \quad \{u_{flex}(t)\} = [\Phi(x, y, z)] \cdot \{q(t)\}$$

A proportional modal damping is applied to the different modes. The amount of damping is a function of the eigenmode frequency.

Except for the FEM model creation, the whole procedure of creating and linking the flexbody into the MBD model is assisted by the FlexPrep utility in Altair MotionView interface. In parallel, the necessary transformation matrices needed for stress (or strain)

recovery from modal coordinates according to Eq. (3) are generated.

$$(3) \quad \{\sigma_{flex}(t)\} = [H]^{-1} \cdot [D] \cdot [\Phi(x, y, z)] \cdot \{q(t)\}$$

In Eq. (3) matrix $[H]$ represents the generalized linear stress-strain relationship (i.e. Hooke's law) in matrix form and matrix $[D]$ contains the derivative operators in space to obtain strain from displacements.

3. RESULTS AND VALIDATION

In order to validate the MBD model, a comparison of in-flight measurement data from selected flight maneuvers is performed side by side with the obtained MBD results (at first only for rigid body simulation) as well as with results from an analytical approach for the same maneuvers.

Besides other instrumented components which were monitored during the Bluecopter flight test campaign, in-flight measurement data for parts of the upper control - the assembly of interest - is available for one rotating control rod and the three boosters for lateral, longitudinal and collective controls.

Whilst the rotating control rod force serves as input load for the MBD analysis, the three boosters, which are directly connected to the main hydraulic actuators on the helicopter, are the last interface in the idealized upper control and therefore the interface of interest for the present investigation.

In-flight measurement data also reveals cyclic and collective actuator strokes, which are implemented in the MBD model accordingly in order to account for the correct swashplate tilt angle corresponding to the considered flight maneuver.

Load results for components between input and output rods cannot be validated due to missing data from the flight test, but it is assumed, that if the cyclic and collective boosters show good correlation between simulation and in-flight measurements, all interfaces in the same control chain indicate valid loads as well.

3.1 Selected flight maneuvers

The stabilized state of two specific maneuvers, namely a pull-up maneuver and a level flight, were selected for the investigation.

The pull-up maneuver was chosen, because it introduces very high loads into the components of the upper control, i.e. loads which are slightly lower than limit load. Since it is a very dynamic flight state, care has to be taken in order to extract the loads from a

properly stabilized maneuver phase in terms of as few as possible corrective control inputs.

The level flight on the other hand is a flight condition with only moderate control loads. Barely any corrective inputs are needed whilst the stabilized level flight is performed. Therefore the extracted in-flight measurement data hardly show any deviation in the five force peaks during one rotor rotation.

Figure 6 shows the pitch link force distribution over one full rotor rotation (over 360° azimuth) of the pitch link connected to the first blade for both maneuvers. This force distribution serves as input for the MBD analysis as described in detail in chapter 2.1.

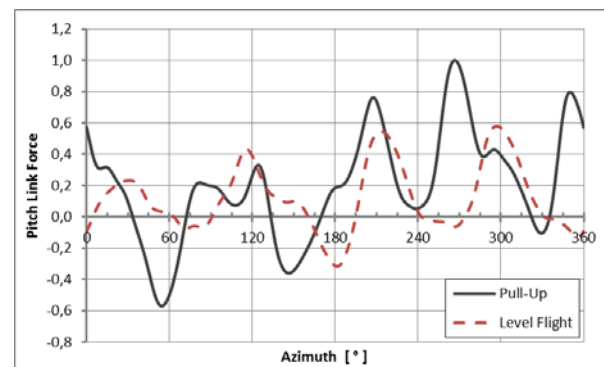


Figure 6: Pitch link force distribution over blade azimuth position (0° equals to tailboom axis)

As expected, the pitch link load indicates higher overall amplitudes during one rotor rotation of the pull-up maneuver compared to the level flight. The pitch angle of the advancing blade is increasing from the drag produced by the up tilting rotor disc, causing a compression of the pitch links. On the retreating blade, a tension load having its maximum at 270° is introduced into the pitch link rods due to a forced decrease of the pitch angle. This phenomenon is caused by the aerodynamic forces acting on the steep airfoil slant after reaching maximum lift at 180° azimuth.

During level flight the retreating blade sees higher pitch link loads compared to the advancing blade as well, but they are not nearly as high as the loads during the same azimuthal position of the blade during the pull-up maneuver. Additionally two almost identical tension maxima appear before and after 270° azimuth.

To conclude, both maneuvers show very different pitch link loads in quality (shape over 360° azimuth), as well as quantity (load minima and maxima). By selecting such different maneuvers, the robustness of the results obtained by the MBD model can be evaluated.

3.2 Comparison of Measurement Results and Calculated Data

The in-flight measurement data of the selected maneuvers is compared to the results of the MBD analysis and analytical calculations. The analytical approach is based on static equilibrium equations comprising the lever ratios of all relevant components of the considered control chain (i.e. lateral, longitudinal or collective axis) in relation to the angle of the swashplate and the azimuth position of all five pitch links. Assumptions on load distribution are made to make the system iso-static.

3.2.1 Pull-Up Maneuver

Figure 7 depicts the load at the collective booster. The spacing of the five maximum and minimum load peaks indicates the 72° phase shift of the rotor blades.

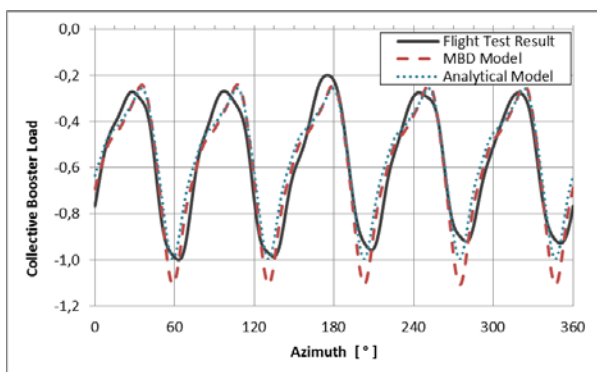


Figure 7: Collective booster load; pull-up maneuver

Looking at the maximum loads of the flight measurement results, one notices almost 10% variance in the data if comparing the load minimum in the beginning of the rotation (~60° azimuth) with the minimum at the end (~350° azimuth) although a nearly stable phase of the maneuver was analyzed as mentioned in chapter 3.1. Obviously the maxima and minima of the rotating control rod forces differ for each rod and blade, which are following with 72° shift. Therefore the MBD results and the analytical approach, which are using only the data of one pitch link for all five blades, does not fit perfectly. The MBD analysis indicates higher absolute loads than the flight test results and analytical considerations, which can be judged as conservative. On the other hand, the minimum absolute booster force calculated analytically and also computed by the MBD method shows slight deviations from the flight test results. The overall accuracy of the analytical model as well as the MBD approach compared to in-flight data can be judged as sufficient for the collective control force prediction.

Figure 8 and Figure 9 depict an even better accuracy between the considered load trends. Despite of slightly varying load amplitudes of the different pitch links from

the flight test data, a very good overall data correlation could be achieved by all simulation approaches for lateral and longitudinal booster loads. A small phase shift of the MBD approach especially during descending lateral booster loads within the course of the rotation is noticeable.

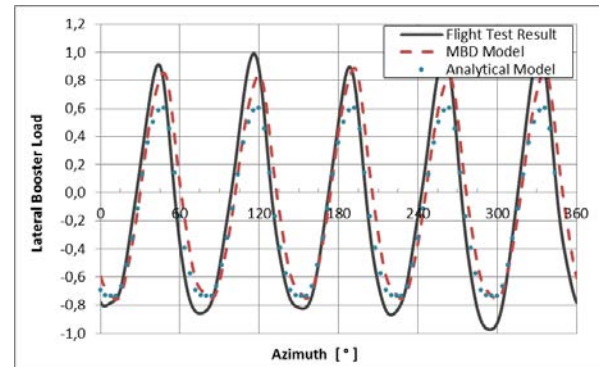


Figure 8: Lateral booster load; pull-up maneuver

In contrary to the collective booster force, lateral and longitudinal booster loads are underestimated by up to 10% with MBD and up to 40% with the analytical approach compared to in-flight data.

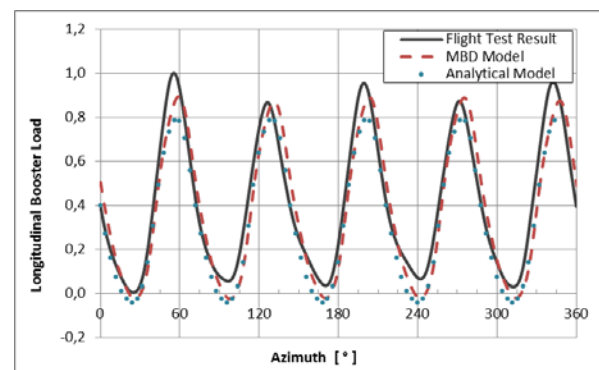


Figure 9: Longitudinal booster load; pull-up maneuver

3.2.2 Level Flight

As expected, the peaks of the collective control force are much more constant over an azimuth of 360° during level flight, than during the pull-up maneuver, as shown in Figure 10. The measured peak load varies by 5% at maximum, resulting in a very good correlation to the numerical and analytical models within the whole azimuth-range.

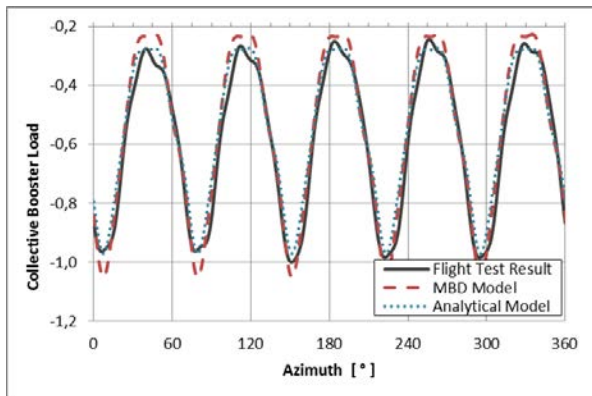


Figure 10: Collective booster load; level flight

As seen before for the collective axis, lateral and longitudinal force correlation with the simulation results is satisfying also for the level flight condition (see Figure 11 and Figure 12).

This time the numerical model overestimates the measured lateral output force. The analytical approach for the lateral axis results in almost identical loads compared to the flight data. Longitudinal axis indicates a slight underestimation of the absolute maximum loads of MBD model and analytical calculation.

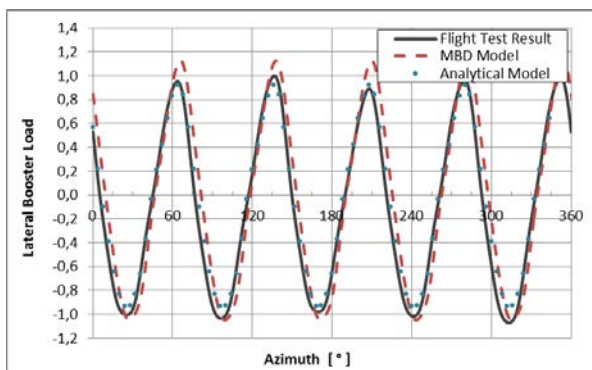


Figure 11: Lateral booster load; level flight

Due to the more regular and stabilized measurement values over the azimuth, the phase shift of the numerical results up to 4° during descending (lateral booster) and ascending (longitudinal booster), load variation over the rotor rotation becomes more obvious. This behavior is expected to be caused by the variation of the pitch link loads, which are not an exact copy of the first pitch control rod repeated five times with 72° shift, as idealized in the models.

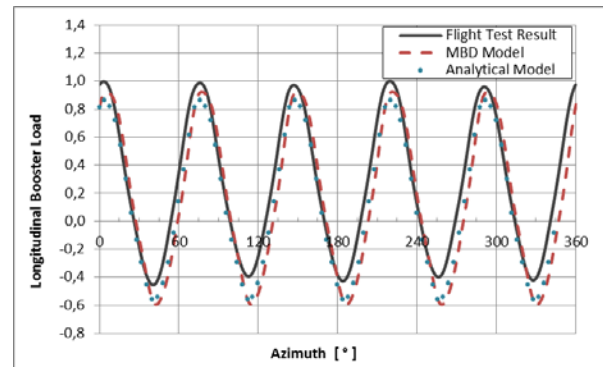


Figure 12: Longitudinal booster load; level flight

3.2.3 Influence of Swashplate Tilting Angle on Booster Loads

Whilst it was a simple adjustment in the MBD model, for the analytical approach great effort had to be spent in order to implement the relation between pitch link input force and booster output load in dependency of the swashplate tilting angle. In order to study the impact of the swashplate tilt on the booster forces, the pull-up maneuver discussed in the previous chapters was analyzed with the swashplate tilting angle according to the measurement results from flight test, and compared to a simulation result with the same input forces, but a leveled swashplate.

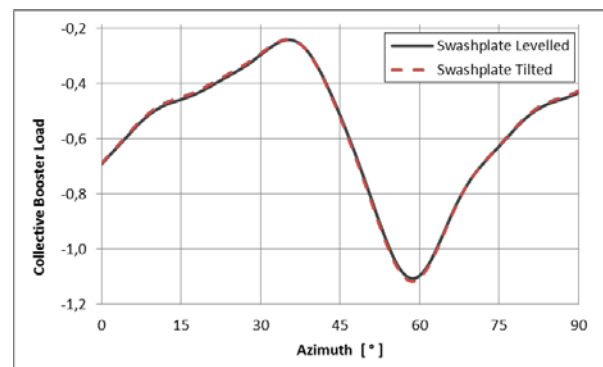


Figure 13: Collective booster load; pull-up maneuver; swashplate positions

Collective booster loads as well as lateral booster loads show close to no variation between the different swashplate tilting angles, which can be seen in Figure 13 and Figure 14. The same applies to the longitudinal booster load, which is not shown for this reason.

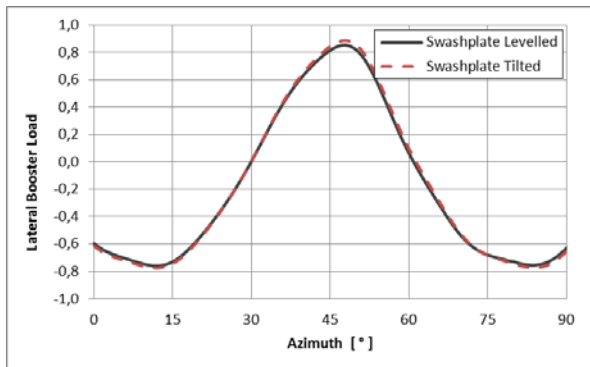


Figure 14: Lateral booster load; pull-up maneuver; swashplate positions

As a result it can be stated, that if only booster loads have to be analyzed, the swashplate position is not relevant for the calculated results. This statement applies only to upper control systems whose design is similar to the one of the Bluecopter.

The tilting of the swashplate will only be relevant for interface load analyses of all components directly connected to the bearing ring and control ring, which have to counteract the lateral forces resulting from the tilt and angled pitch link rods.

3.2.4 Influence of Flexible Bodies on Booster Loads

In previous chapters the numerical results were based on a rigid modeling of the upper control. As described in chapter 2.3, four rigid bodies were now replaced by flexbodies; namely cyclic levers and (collective) forked lever, as well as the bearing ring of the swashplate, in order to investigate their influence on the output forces of interest.

The results of the analysis are compared to the previously gathered data from the analysis of the pull-up maneuver rigid MBD simulation and flight test results as shown in Figure 15.

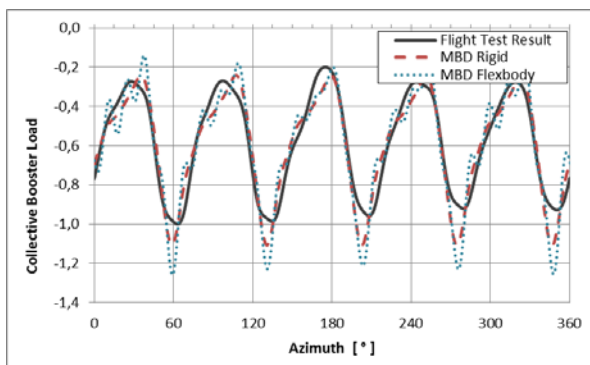


Figure 15: Collective booster load - comparison of the different MBD approaches (with rigid & flexible bodies) with in-flight data

The dotted green diagram represents the results obtained from the simulation with flexbodies. Besides a further overshooting of the maximum absolute force compared to the results obtained with the rigid MBD model, an oscillation of the output force during a less loaded state is clearly visible.

Further analysis of this phenomenon revealed that the flexible forked lever causes this behavior. As it is less present at the lateral booster lever and hardly visible in the plotted loads from the longitudinal booster lever, it is expected to be a result of the constraints fixing the forked lever to sliding sleeve and especially the bearing block. Further analysis and tuning of the model is necessary in order to eliminate these unrealistic load oscillations.

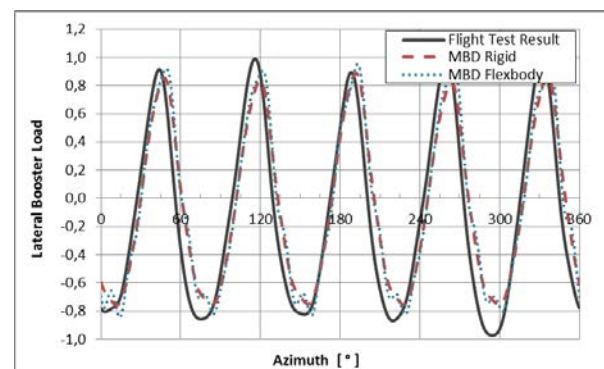


Figure 16: Lateral booster load; comparison of MBD approaches with in-flight data

The lateral booster load output plot of the flexbody analysis shows better correlation with flight test results, in terms of load amplitude, in comparison to the rigid analysis. Minor oscillations are observed in the negative load range only (see Figure 16).

The longitudinal booster force output from the flexbody simulation shows basically no oscillations (see Figure 17). Neither in the force maxima, nor in the force minima, measurable deviations from the flexbody results compared to the rigid bodies are present. Since the oscillations only occur in the negative load range of the lateral booster, a possible reason for this behavior is expected to be the different load ratio of lateral and longitudinal forces. Despite their comparable amplitude value, the lateral forces are oscillating around zero whilst the longitudinal loads have a swelling character.

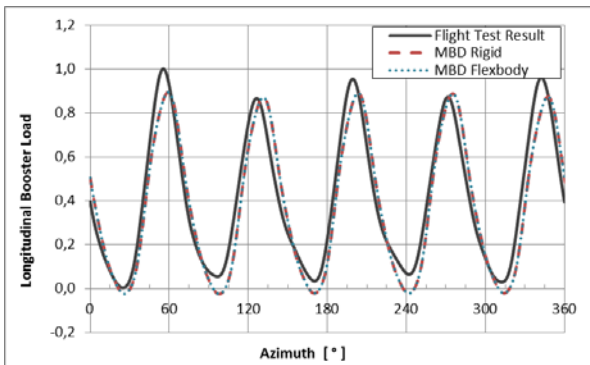


Figure 17: Longitudinal booster load; comparison of the different MBD approaches (with rigid & flexible bodies) with in-flight data

For the analyzed interfaces only minor benefits in terms of accuracy compared to flight test data could be achieved by the use of flexible bodies in the MBD simulation. Especially for the collective booster the results are more conservative compared to the same simulation with rigid bodies.

The use of flexbodies for the first load estimation in the early design phase of a development project is therefore not recommended. The typical scenario for the introduction of flexbodies would be recommended mainly for detailed sizing purposes, i.e. after the initial geometrical parameters are frozen. Additionally the flexbodies allow for a quick evaluation of stress hotspots within the preliminary component geometries. Moreover, the deformations under load can be studied, and consequently critical component positions can be identified in order to avoid clearance issues especially under limit load conditions. Flexbody-based analyses can also help evaluating the in-service damages and defining the corresponding repair limits.

4. CONCLUSION

The upper control assembly of the Bluecopter prototype rotorcraft has been investigated by means of a MBD model. Objective of this study is to develop a methodology to accurately predict the interface loads, deformations and stress distribution in the different components of the upper control.

The two exemplary flight maneuvers have been analyzed by MBD and results have been validated by comparison to analytical results and flight measurement data.

A good correlation between experimental and simulation results was obtained in terms of loads for lateral, longitudinal and collective boosters in the kinematic flight control chain. It could be shown, that for first load estimations an analytical approach is fully sufficient and MBD simulation could not improve the

load prediction considerably for the investigated interfaces. The advantage of the MBD model arises, if interfaces between pitch links and booster rods have to be analyzed, which is not possible with the described analytical method.

Flexible bodies have been introduced in the MBD model mainly in order to accurately predict the deformations and stress distributions in the most critical components. A comparison of the booster forces with the rigid model and in-flight measurements did not indicate improved accuracy.

The advantage of this approach is the possibility to perform a more accurate fatigue calculation by considering the real stress tensor variations for many different maneuvers, without the need to perform flight measurements for every single flight state. In addition, this methodology allows for stress-driven weight optimization.

Additional investigations will be performed in the future with respect to joint properties and the rotational speed of the rotor. The main goal is to include friction in the joints, check the influence of eventual damages in the kinematic chain and check the influence of a non-uniform rotor speed on the loads.

The methodology shown in this paper is currently used at AHD for steady flight state analysis only. The same approach might be extended to simulate transient maneuvers in the future as well.

5. REFERENCES

- [1] M. Bebesel, A. D'Alascio, S. Schneider, S. Guenther, F. Vogel, C. Wehle, D. Schimke, "Bluecopter Demonstrator – An approach to eco-efficient helicopter design" European Rotorcraft Forum, 2015
- [2] R.R. Craig, M.C.C. Bampton "Coupling of substructures for dynamic analysis" AIAA Journal, 1965 - 6(7):678-85
- [3] R.R. Craig "Structural dynamics - an introduction to computer methods" John Wiley & Sons, 1981